Lung Cancer 131 (2019) 112–121

Contents lists available at ScienceDirect

Lung Cancer

journal homepage: www.elsevier.com/locate/lungcan

FGFR4 increases EGFR oncogenic signaling in lung adenocarcinoma, and their combined inhibition is highly effective

Alvaro Quintanal-Villalonga[a,b], Sonia Molina-Pinelo[c,g], Patricia Yagüe[a,g], Ángela Marrugal[a], Laura Ojeda-Márquez[a,g], Rocío Suarez[a,g], Santiago Ponce-Aix[d,g], Ana Belén Enguita[e], Amancio Carnero[c,g], Irene Ferrer[a,g,**,1], Luis Paz-Ares[a,d,f,g,*,1]

[a] H120-CNIO Lung Cancer Clinical Cancer Research Unit, Fundación de Investigación Biomédica i + 12 & Centro Nacional de Investigaciones Oncológicas (CNIO), Madrid, Spain
[b] Program in Molecular Pharmacology, Memorial Sloan Kettering Cancer Center, New York, New York, United States
[c] Instituto de Biomedicina de Sevilla (IBIS) (HUVR, CSIC, Universidad de Sevilla), Sevilla, Spain
[d] Medical Oncology Department, Hospital Universitario Doce de Octubre & Centro Nacional de Investigaciones Oncológicas (CNIO), Madrid, Spain
[e] Pathological Anatomy Department, Hospital Universitario Doce de Octubre & Centro Nacional de Investigaciones Oncológicas (CNIO), Madrid, Spain
[f] Medical School, Universidad Complutense, Madrid, Spain
[g] CIBERONC, Madrid, Spain

ARTICLE INFO

Keywords:
FGFR4
EGFR
TKIs
Treatment resistance
Combination treatment

ABSTRACT

Objectives:Lung adenocarcinoma accounts for approximately half of lung cancer cases. Twenty to 50% of tumors of this type harbor mutations affecting epidermal growth factor receptor (EGFR) expression or activity, which can be therapeutically targeted. EGFR inhibitors in this context exhibit high efficacy and are currently used in the clinical setting. However, not all adenocarcinomas harboring EGFR mutations respond to therapy, so predictive biomarkers of therapeutic outcomes, as well as novel therapies sensitizing these tumors to EGFR inhibition, are needed.

Materials and methods:We performed *in vitro* gene overexpression/silencing and tumorigenic surrogate assays, as well as *in vitro* and *in vivo* combination treatments with Fibroblast Growth Factor Receptor (FGFR)/EGFR inhibitors. At the clinical level, we determined FGFR4 expression levels in tumors from patients treated with EGFR inhibitors and correlated these with treatment response.

Results:We describe a cooperative interaction between EGFR and FGFR4, which results in their reciprocal activation with pro-oncogenic consequences *in vitro* and *in vivo*. This cooperation is independent of EGFR activating mutations and increases resistance to different EGFR inhibitors. At the therapeutic level, we provide evidence of the synergistic effects of the combination of EGFR and FGFR inhibitors in high FGFR4-expressing, EGFR-activated tumors *in vitro* and *in vivo*. Correlated with these results, we found that patients treated with EGFR inhibitors relapse earlier when their tumors exhibit high FGFR4 expression.

Conclusions:We propose a novel predictive biomarker for EGFR-targeted therapy, and a highly efficacious combinatory therapeutic strategy to treat EGFR-dependent; this may may extend the use of appropriate inhibitors beyond EGFR-mutated adenocarcinoma patients.

1. Introduction

Lung adenocarcinoma is the most prevalent type of pulmonary malignancy, accounting for approximately half of lung cancer cases [1–4]. A high percentage of adenocarcinomas harbour known driver molecular aberrations, some of which are therapeutically targetable. This is the case of EGFR activating mutations, accounting for up to 20% of lung adenocarcinoma cases in Caucasian cohorts and in up to

* Corresponding author at: Head of Medical Oncology Department, Hospital Universitario 12 de Octubre, Associate Professor, Universidad Complutense de Madrid, Av de Andalucia s/n, 28041 Madrid, Spain.
** Corresponding author at: H12O-CNIO Lung Cancer Clinical Research Unit, Research Institute of Hospital 12 de Octubre (i + 12), Av. de Córdoba s/n, Madrid 28041, Spain.
E-mail addresses: ireneferrersan@gmail.com (I. Ferrer), lpazaresr@seom.org (L. Paz-Ares).
[1] These authors contributed equally to this work.

https://doi.org/10.1016/j.lungcan.2019.02.007
Received 29 August 2018; Received in revised form 4 February 2019; Accepted 7 February 2019

30–50% of patients of Asian origin [5,6]. The development of small molecule inhibitors targeting the EGFR receptor has improved treatment outcomes in patients with tumors possessing these mutations [7–10]. However, the use of such inhibitors is currently restricted to adenocarcinomas with known EGFR activating mutations. Thus, tumors exhibiting high constitutive EGFR activation mediated by either unknown EGFR mutations or by other molecular mechanisms, which may also benefit from these therapies, are not candidates for treatment with EGFR inhibitors. Furthermore, not all tumors harbouring known EGFR-activating mutations respond to EGFR inhibitors [3,11–13]. Therefore, the discovery of novel biomarkers predicting EGFR therapy efficacy, as well as the identification of therapies achieving higher efficacy against EGFR signalling-dependent tumors is an unmet clinical need.

Similar to EGFR, another receptor tyrosine kinase (RTK), fibroblast growth factor receptor 4 (FGFR4), is gaining attention in the lung cancer setting. The protein expression of this receptor has been recently associated with a negative impact on lung cancer prognosis, supporting the idea that FGFR4 could have oncogenic potential in these tumors as well [14]. Furthermore, FGFR4 has also been reported to be occasionally mutated in lung adenocarcinoma [15–17] leading to activation of oncogenic signaling pathways with impact on patient survival [18,19]. Expression of FGFR4 was found to be upregulated in EGFR-transformed mouse embryonic fibroblasts (MEFs) compared to MEFs transformed by other methods [20], sugesting a potential cooperative interaction between both RTKs. However, the oncogenic role of FGFR4 in the context of EGFR-dependent lung adenocarcinoma has thus far not been addressed.

2. Materials and methods

2.1. Cell lines

All cell lines (**Supplementary Table 1**) were purchased from the American Type Culture Collection (ATCC) just prior to commencing this work, with the exception of H1437 and H3122, which were kindly provided by Dr. Maina and Dr. Koivunen, respectively. All cell lines were authenticated and regularly tested for mycoplasma.

2.2. Transfections

Cell lines were transfected with TransIT-X2 Transfection Reagent (Mirus). The FGFR4 (RG204230) cDNA clone was obtained from Origene in the pCMV6 plasmid (PS100001). To overexpress wild type EGFR and L858R/T790 M EGFR, the pBABE EGFR (#11,011), pBABE EGFR (L858R/T790 M) (#32,073) and empty pBABE (control empty plasmid, #51,070) plasmids were obtained from Addgene. For FGFR4 silencing, short hairpin (sh)RNAs in the pRS plasmid were purchased from Origene (TR320356). The appropriate selection antibiotic was used to select positive transfected clones, which were then pooled in a monolayer, and maintained under continuous selective pressure. For shRNA silencing, two independent shRNAs were used to avoid off-target effects.

2.3. Growth factor stimulation

Cells were serum-starved for five hours to induce basal phosphorylation levels and then stimulated with serum-free medium containing FGF19 (100 ng/mL, Immunostep) or EGF (50 ng/ml, Immunostep), or with complete medium (10% Fetal Bovine Serum (FBS)) for 15 min. Protein extracts were subsequently obtained as indicated below.

2.4. Surrogate assays

Clonogenicity and soft agar assays were performed as indicated in [21]. For growth curves, cells (3500 per well) were seeded in 12-well culture plates in complete growth medium. At least three replicate growth curves were analyzed for each experiment. The cells for the first point of the curve (day 0) were fixed with a 0.5% glutaraldehyde solution 24 h after seeding. Every two days, a plate of cells corresponding to a point on the curve was fixed, and the cells were stored in PBS at 4 °C until the sample for the last point of the curve was fixed. Cells were then stained with a 1% crystal violet solution (crystal violet dissolved in a 20% acetic acid/water solution) and washed. Absorbance was measured at 595 nm in a VICTOR plate reader (PerkinElmer). Values were normalized to the day 0 absorbance and plotted versus time.

2.5. Co-immunolocalization

Cells were fixed with 4% paraformaldehyde and blocked with 1% BSA in 0.1% Triton X-100 in PBS for 1 h at room temperature. They were then incubated with mouse anti-EGFR (#MA5-13269, ThermoFisher) and rabbit anti-FGFR4 (#8562, CST) antibodies at a 1:100 dilution in blocking buffer for 3 h at room temperature and then labeled with Alexa Fluor® 488 Goat Anti-Rabbit IgG (#R37116, ThermoFisher) and Alexa Fluor® 555 Donkey Anti-Mouse IgG secondary antibodies (#A-31570, ThermoFisher) at a dilution of 1:250 for 1 h at room temperature. Images of 15–20 cells per condition were taken with an SP5-WLL confocal microscope.

2.6. Proximity ligation assay (PLA)

PLA was performed using the Duolink Kit (#DUO92102, Sigma), following the manufacturer's instructions and using the primary antibodies described above for the immunolocalization assays.

2.7. Cell line treatments

The inhibitory concentration 50 (IC50) was calculated by treating cells seeded in 96-well plates with a range of concentrations of each inhibitor under assay for 96 h. Cells were then fixed and stained with crystal violet (0.1%). Then, cristal violet was diluted in 20% acetic acid solution. Absorbance measured at 595 nM, which is correlated to the number of cells in each well, was quantified and analyzed as in [22]. For combination treatments, the approximate mean value of IC20 FGFR inhibitor concentration and this concentration doubled were combined with the different EGFR inhibitor concentrations to determine the IC50 value for the EGFR inhibitor in combination with the FGFR inhibitor. The synergistic relationship between both kinds of inhibitors was calculated following the Chou-Talalay method as in [23]. To study the effect of treatments on the downstream signaling of cell lines, cells were treated for 24 h with the IC50 concentration of erlotinib, alone or in combination with the IC50 of AZD4547, and protein extracts were obtained.

2.8. Cell line xenografts and in vivo treatments

For cell line xenografts, cell were diluted in PBS and then mixed with Matrigel (1:1) A 150 µl aliquot (2×10^6 cells) of the mixture was injected into one flank of each of 4–8 6-week-old female athymic nude mice. The number of mice used per group was based on previous experiments in the laboratory.

Tumors were measured twice a week after injection; when tumor volume had reached 150-200 mm^3, mice were randomized into groups with similar mean tumor size and standard deviation. Mice were sacrificed at the end of treatment and tumor samples harvested and stored.

Erlotinib, AZD4547, or a combination of the two, was administered on five consecutive days each week at a concentration of 50 mg erlotinib/kg/day for the H1975 models, and 25 mg erlotinib/kg/day for the HCC827 models. AZD4547 was administered at a concentration of 5 mg/kg/day. The duration of the treatments was 5 weeks, unless rapid tumor growth necessitated an earlier endpoint.

Experimenter blinding was achieved in these experiments by having one person treat the animals and a different person measure the tumors and process the data.

2.9. Immunoblot

Western blot was performed as indicated in [24]. The following antibodies were used: FGFR4 (#8562, Cell Signaling), pFGFR4 (MBS856043, MyBiosource), AKT (#9272, Cell Signaling), pAKT (#9271, Cell Signaling), p42/p44 (#9102, Cell Signaling), p-p42/p44 (#9101, Cell Signaling), STAT3 (#9139, Cell Signaling), pSTAT3 (#9145, Cell Signaling), α-tubulin (T9206, Sigma), β-actin (#A5316, Sigma), EGFR (#4267, Cell Signaling), and pEGFR (#2234, Cell Signaling). HRP-conjugated anti-rabbit and anti-mouse secondary antibodies were purchased from Cell Signaling. All primary antibodies had been previously validated in this specific assay and their specificity tested with adequate control samples. Western blot images with a high number of lanes were assembled from blots run in parallel and with a common reference sample on both gels.

2.10. Co-immunoprecipitation assays

Co-immunoprecipitation was performed using the EZ View Red Protein G Affinity Gel (#E3403, Sigma). Protein extracts were prepared in HEPES 50 mM, NaCl 150 mM and n-octylglucoside 1% and supplemented with a protease inhibitor cocktail (cOmplete Mini EDTA-free, Roche) and a phosphatase inhibitor cocktail (PhosSTOPEASYpack, Roche). 2 mg protein aliquots were precleared and incubated with antibody-conjugated beads. The EGFR (#4267, Cell Signaling) antibody was used 1:100 for the immunoprecipitation, and an equal amount of anti-IgG isotype control antibody (#3900, Cell Signaling) was used as a negative control. Immunocomplexes were denatured by boiling in Laemmli buffer and a western blot protocol was performed to confirm the immunoprecipitation and to assess the co-immunoprecipitation of FGFR4.

2.11. RNA extraction and mRNA expression analysis

RNA extraction of FFPE patient tumor tissues was performed with the RecoverAll Extraction Kit (Life Technologies, #AM1975). RNA samples were reverse transcribed with the TaqMan Reverse Transcription Kit (Life Technologies). Gene expression was analyzed after a preamplification step performed with the TaqMan Preamp Master Mix Kit (Applied Biosystems, #4,384,266) by using TaqMan probes from Life Technologies: Hs01106908_m1 FAM (FGFR4) and Hs99999907_m1 FAM (B2M). B2M expression was used to normalize the expression data.

2.12. Public database of cancer cell lines: sensitivity to EGFR inhibitors

Information on sensitivity to the EGFR inhibitors lapatinib and erlotinib of the cell lines used and of FGFR4 mRNA expression was obtained from the Cancer Cell Line Encyclopedia (CCLE) database (https://portals.broadinstitute.org/ccle/home).

2.13. Clinical samples

The study included a cohort of 87 subjects diagnosed with advanced (stage III-IV) non-small-cell lung carcinoma (NSCLC) from the University Hospital 12 de Octubre (Madrid, Spain) given erlotinib or gefitinib as a first-, second-, third- or furtherline treatment. Tumor samples were sent the Hospital's pathology laboratory for diagnosis and were prepared for storage by formalin fixation and paraffin embedding. Inclusion criteria were: (1) Confirmed NSCLC diagnosis, (2) access to patient clinical information, and (3) availability of tumour tissue obtained by surgical resection. For the tumor marker prognostic study, the REMARK [25] reporting guidelines were followed. Baseline characteristics of the patient cohort are summarized in **Supplementary Table S2.**

2.14. Study approval

Written informed consent was provided by all patients. The project was approved by the Research Ethics Committee of the Hospital Universitario 12 Octubre (Madrid, Spain) (CEI 16/297).

Procedures involving animals were approved by the Animal Protection Committee of the Comunidad Autónoma de Madrid (Approval ID: PROEX134/16).

2.15. Statistics

In vitro data are represented as the mean ± standard deviation to indicate variation within each group of data. Statistical analysis was performed with the SPSS statistical package (v19, IBM). The *in vitro* and *in vivo* experiments were analyzed using an unpaired non-parametric Mann-Whitney's U test or Student's *t*-test. Values of $p < 0.05$ were considered significant. The Kaplan-Meier method was used for survival analyses of the clinical data and cell line xenograft experiments, with a Cox proportional hazards model used to adjust for explanatory variables, following which p-values were obtained. Overall survival (OS) was defined as the length of time from the date of diagnosis to the date of the last medical record. Progression-free survival (PFS) was defined as the length of time from the date of diagnosis to the date of relapse. A type II ANOVA was used to analyze differences in survival among groups. To obtain the hazard ratio values, the Cox proportional hazards model was used.

3. Results

3.1. FGFR4 overexpression increases EGFR signaling and oncogenic capacities in EGFR-mutated lung adenocarcinoma cell lines

FGFR4 and EGFR protein expression, as well as EGFR activation were determined in a panel of lung adenocarcinoma and immortalized lung epithelial cell lines (Fig. 1A**, SupplementaryTable S1**). As expected, high EGFR activation was observed in the EGFR-mutated cell lines, but also in two other cell lines, H1781 and Calu-3. However, EGFR mutational profiling of these two cell lines revealed no EGFR activating mutation in either cell line (data not shown).

To address the role of FGFR4 in the EGFR-mutated adenocarcinoma setting, FGFR4 was overexpressed in two cell lines harbouring two different EGFR activating mutations (**SupplementaryTable S1**). FGFR4 overexpression in either cell line led to increased growth and clonability capacities in all cell lines tested, and to increased soft agar colony formation in the only cell line used by us that exhibited anchorage-independent growth, HCC827, as compared to the respective control cell lines (Fig. 1**B-C and Supplementary Figure S1 A**). After analyzing the activation of some RTK-related signaling pathways in these cell lines (Fig. 1D), we observed increased EGFR, and slightly elevated STAT3 and AKT activation in the FGFR4-overexpressing cells after serum deprivation. When cells were stimulated with EGF, EGFR activation was higher in the FGFR4-overexpressing cells, and increased ERK activation was also observed under these conditions for the HCC827 cell line. Of note, FGFR4 activation occurred in parallel with EGFR activation. Moreover, when these cells were stimulated with the FGFR4 specific factor FGF19 (Fig. 1E), activation of both FGFR4 and EGFR was observed. These results suggested a cooperative interaction between the two RTKs.

To address the relevance of this potential cooperation *in vivo*, these cell lines were xenografted into immunodeprived nude mice. Tumor size determination as a function of time revealed increased tumor growth in the FGFR4-overexpressing xenografts (Fig. 1F).

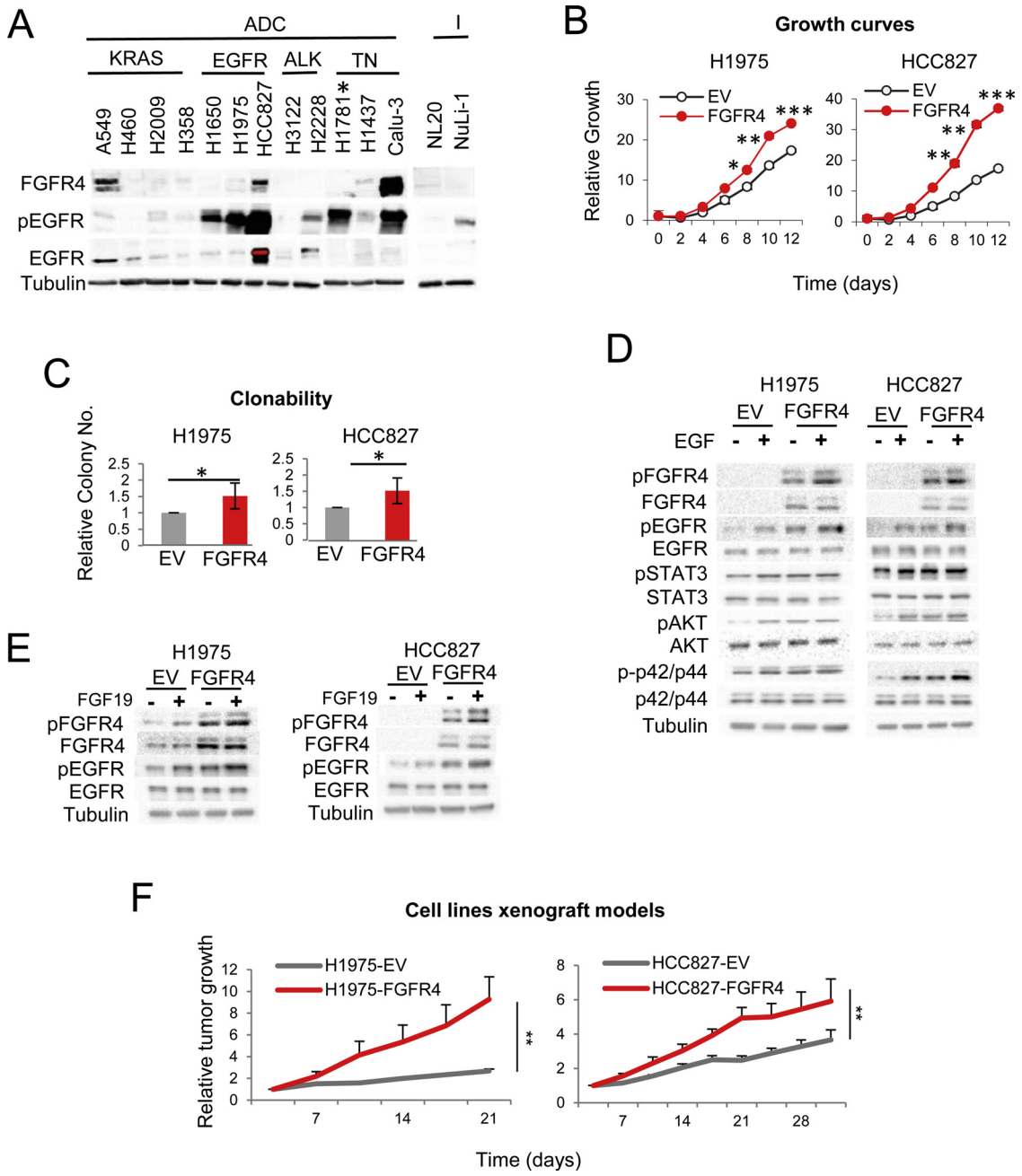

Fig. 1. Effect of FGFR4 overexpression on tumorigenesis of EGFR-mutation driven lung adenocarcinoma cell lines. (A) Characterization of FGFR4 and EGFR protein expression and EGFR activation in a panel of lung cell lines. (B) Growth curves in 10% FBS and (C) clonability assays of FGFR4-overexpressing EGFR-mutated adenocarcinoma cell lines. (D) Western blotting of the activation of the EGFR and RTK-related signaling pathways in the FGFR4-overexpressing, EGFR-mutated H1975 and HCC827 lung adenocarcinoma cell lines compared to the empty vector-containing cell lines after stimulation with recombinant human epidermal growth factor (EGF). (E) Western blotting of the activation of the EGFR and RTK-related signaling pathways in FGFR4-overexpressing H1975 and HCC827 cells after stimulation with the FGFR4-specific FGF19. (F) Growth assessment of the tumors generated by FGFR4-overexpressing H1975 and HCC827 cell line xenografts. The colony number is shown for the clonability and soft agar assays. All values were normalized to the empty vector control, and the mean of all the normalized replicates is presented. For western blotting, cells were serum-starved for 5 h prior to protein extraction. For the growth factor-stimulated conditions, serum-starved cells were stimulated with serum-free medium containing FGF19 fifteen minutes prior to protein extraction. All experiments were repeated a minimum of 3 times in the laboratory. For growth curves and western blots, a representative figure/image is shown. On the growth curves, the means and standard deviations of the technical replicates are shown. p-values were obtained with the two-sided Mann-Whitney U test and are indicated by asterisks (* $p < 0.05$; ** $p < 0.01$; *** $p < 0.001$). ADC = Adenocarcinoma, I = Immortalized, KRAS = KRAS-mutated, EGFR = EGFR-mutated, ALK = AlK translocation, TN = Triple negative (referring to the absence of KRAS, EGFR and ALK alterations). EV = Empty vector control, FGFR4 = FGFR4-overexpressing. *In the H1781 cell line, referred to as EGFR wild type in the literature (**Supplementary Table S1**), the EGFR-activating L858R mutation was detected. To assess the expression of these proteins in the cell lines, different blots were performed in parallel with an internal reference sample and the assembled images are shown (For interpretation of the references to colour in this figure legend, the reader is referred to the web version of this article).

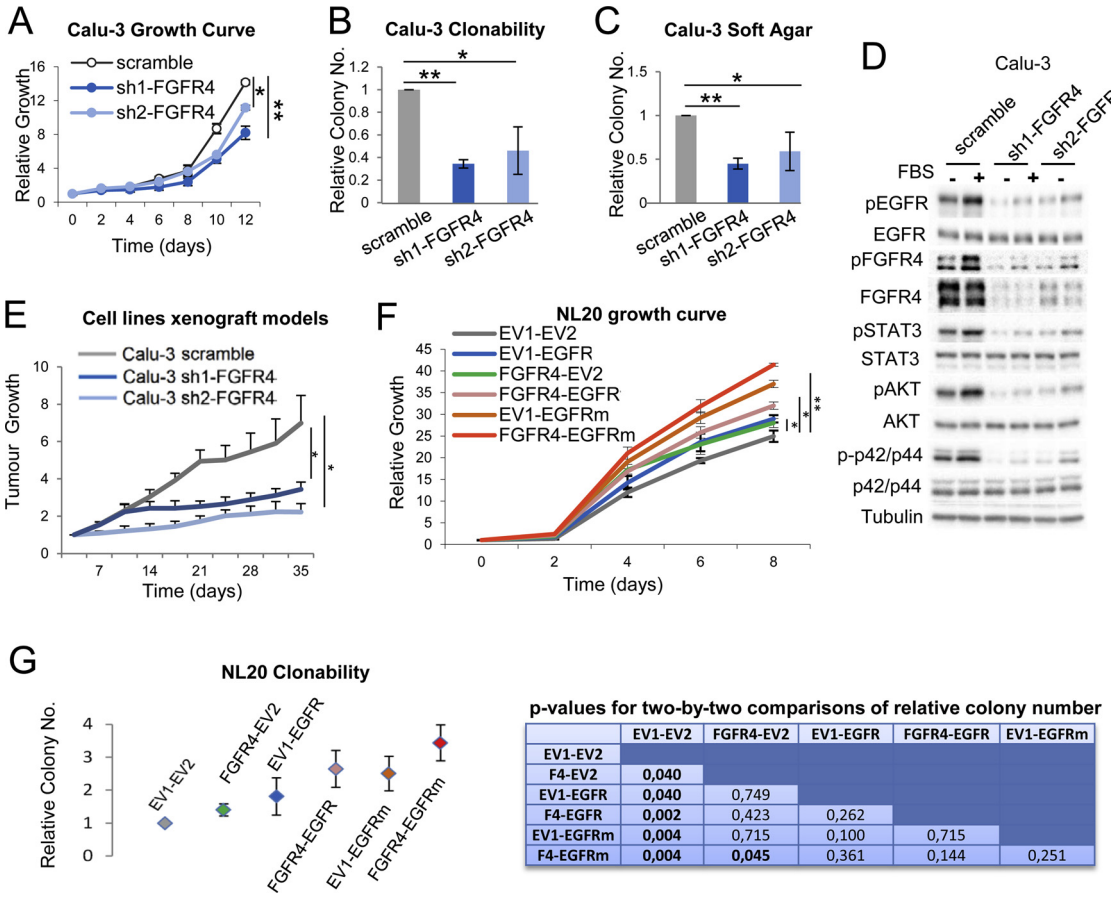

p-values for two-by-two comparisons of relative colony number

	EV1-EV2	FGFR4-EV2	EV1-EGFR	FGFR4-EGFR	EV1-EGFRm
EV1-EV2					
F4-EV2	0,040				
EV1-EGFR	0,040	0,749			
F4-EGFR	0,002	0,423	0,262		
EV1-EGFRm	0,004	0,715	0,100	0,715	
F4-EGFRm	0,004	0,045	0,361	0,144	0,251

Fig. 2. Oncogenic cooperation of FGFR4 with mutated and wild type activated EGFR. Growth curves in 10% FBS (A), clonability (B) and soft agar assays (C) after FGFR4 silencing in the Calu-3 adenocarcinoma cell line, which harbors constitutively activated EGFR. (D) Western blotting of the activation of the EGFR and RTK-related signaling pathways in FGFR4-silenced Calu-3 cells compared to scrambled vector-expressing cells after stimulation with FBS. (E) Growth assessment of the tumors generated by the FGFR4-silenced Calu-3 adenocarcinoma cell line xenografts in immunodeprived mice. Growth curves in 10% FBS (F) Growth curves in 0.5% FBS for NL20 cell lines overexpressing FGFR4 with or without co-expression of wild type or L858R/T790 M EGFR. (G) Clonability assays of the entire panel of NL20 cell lines generated. For growth curves, a representative figure/image is shown. On the growth curves, the mean and standard deviation for the technical replicates are shown. The colony number is shown for the clonability. All the values were normalized to the empty vector control, and the mean of all the normalized replicates is presented. For western blots, a representative image is shown. p-values were obtained with the two-sided Mann-Whitney U test and are indicated by asterisks (* $p < 0.05$; ** $p < 0.01$; *** $p < 0.001$). Scramble = scrambled shRNA control, shFGFR4 = FGFR4 shRNA, FBS = fetal bovine serum, EV1 = empty vector 1, EV2 = empty vector 2, F1 = FGFR4, EGFR = wild type EGFR, EGFRm = L858R/T790 M mutant EGFR (For interpretation of the references to colour in this figure legend, the reader is referred to the web version of this article).

3.2. FGFR4-EGFR cooperation is independent of EGFR-activating mutations

In our cell line panel, the wild type EGFR adenocarcinoma cell line Calu-3 showed high levels of EGFR activation and FGFR4 protein expression (Fig. 1A). Surrogate assays indicated that FGFR4 silencing in this cell line decreased oncogenicity relative to the control (Figs. 2**A-C and Supplementary Figure S1B**). Western blot analysis showed that FGFR4 silencing in Calu-3 cells decreased the activation of EGFR, STAT3, AKT and p42/p44 compared to the control cell line (Fig. 2D), while xenografts of these cell lines in immunodeprived mice showed decreased tumor growth after FGFR4-silencing (Fig. 2E). These results indicate that FGFR4 expression could contribute to the high level of EGFR activation in this cell line, and suggest that the FGFR4-EGFR interaction is not exclusive to cells bearing activating EGFR mutations.

To further confirm the latter observation, FGFR4 was co-overexpressed with different EGFR variants (wild type and L858R/T790 M EGFR) in the immortalized epithelial lung cell line NL20 and surrogate assays were performed. FGFR4 overexpression further increased the oncogenic abilities induced by either EGFR variant (Figs. 2**F-G**). Correlating with these phenotypes, EGFR, STAT3, AKT and p42/p44 signaling activation was further increased by FGFR4 overexpression, as compared to the conditions of overexpression of either EGFR variant (**Supplementary Figure S1C**). These results suggested that the co-operation between FGFR4 and EGFR occurs independently of the presence of EGFR activating mutations.

3.3. Interaction between FGFR4 and EGFR occurs at the physical level

Co-immunofluorescence assays in the FGFR4- and EGFR-overexpressing NL20 cell line showed a partial co-localization between both RTKs at the cell membrane (Fig. 3A). In addition, we observed that FGFR4 co-immunoprecipitated with EGFR in the high FGFR4- and EGFR-expressing cell line Calu-3 (Fig. 3B), while the interaction between both proteins was further confirmed by Proximity Ligation Assay (PLA, Fig. 3C) results. Taken together, these findings suggested that the cooperative effects of both receptors may occur through a physical interaction between them.

3.4. Combined treatment with EGFR and FGFR inhibitors shows high efficacy in FGFR4-overexpressing EGFR-activated cell lines

We found that EGFR-activated, FGFR4-overexpressing cell lines exhibited higher resistance to two different EGFR inhibitors, erlotinib and osimertinib, and higher sensitivity to two selective FGFR inhibitors,

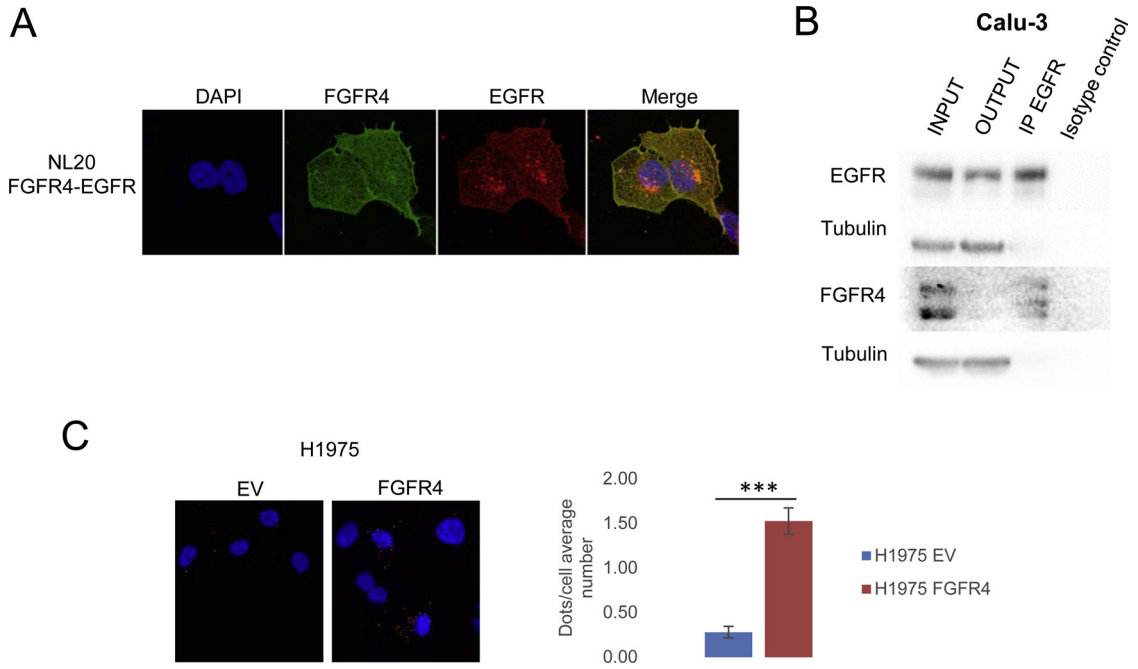

Fig. 3. Interaction of EGFR with FGFR4. (A) Co-immunolocalization assays of EGFR and FGFR4 in the NL20 cell lines overexpressing these genes. (B) Co-immunoprecipitation of EGFR with FGFR4 in the Calu-3 cell line. (C) Proximity ligation assay (PLA) demonstrating the close interaction between EGFR and FGFR4 in control and FGFR4-overexpressing H1975 cell lines. Representative images of the assay are shown (left panel). The presence of red dots in this assay is indicative of the interaction between both receptors. Graph (right panel) shows the average number of dots per cell +/- SEM. EV = Empty vector, FGFR4 = FGFR4-overexpressing, EGFR = EGFR-overexpressing A minimum number of 15 independent images was captured in the immunofluorescence assays, and representative images for each condition are shown. The co-immunoprecipitation assays were independently reproduced 3 times and a representative blot is shown. INPUT = protein sample before immunoprecipitation performance, OUTPUT = protein sample after the immunoprecipitacion was carried out. p-values were obtained with the two-sided t-test and are indicated by asterisks (* $p < 0.05$; ** $p < 0.01$; *** $p < 0.001$) (For interpretation of the references to colour in this figure legend, the reader is referred to the web version of this article).

BGJ398 and AZD4547, as compared to control cell lines However, these effects were not reproduced in three other adenocarcinoma cell lines with no EGFR activation (Fig. 4**A and Supplementary Figures S1D and S2A**). In agreement with our results, high FGFR4 expression correlated with increased resistance to different EGFR inhibitors in lung adenocarcinoma from the Cancer Cell Line Encyclopedia database (**Supplementary Figure S2B**).

In an attempt to address the EGFR-FGFR4 cooperativity *in vitro* from a therapeutic perspective, we treated the EGFR-activated, FGFR4-overexpressing cells with all possible combinations of the EGFR and FGFR inhibitors mentioned above, to measure the effect on cell viability of the dual inhibiton of both receptors. We observed that dual EGFR-FGFR inhibition was synergic, but only in the FGFR4-overexpressing cells (Fig. 4B). As the combination of erlotinib and AZD4547 showed the strongest effect, this inhibitor pair was chosen for further experiments.

Next, we assessed oncogenic signalling in erlotinib/AZD4547-treated H1975 and HCC827 cell lines (Fig. 4C). In the FGFR4-overexpressing cell lines, the combination treatment was more effective than erlotinib alone at inhibiting EGFR signaling. Similar effects were observed for p42/p44. In the HCC827 cell line, dual FGFR-EGFR inhibiton also caused further abrogation of AKT signaling compared to that seen with erlotinib alone, but no such effects were observed in the H1975 cell line. Regarding the STAT3 pathway, erlotinib monotherapy caused an increase in pSTAT3 levels, an effect already described in the literature for EGFR and other targeted therapies leading to therapy resistance [26,27]. However, this STAT3 overactivation was partially abrogated when AZD4547 was co-administered with erlotinib.

3.5. Combined FGFR/EGFR inhibition shows high efficacy in EGFR-activated, FGFR4-overexpressing cell lines in vivo

The efficacy of FGFR and EGFR inhibition, in monotherapy and in combination, was assessed in xenografts of FGFR4-overexpressing H1975 and HCC827 cell lines (Figs. 5**A-B**). At the monotherapy level, and in agreement with our *in vitro* results, FGFR4-overexpressing HCC827 cells exhibited higher resistance to erlotinib than their control counterparts. This effect was not observed for H1975, probably due to the intrinsic erlotinib resistance mutation in this cell line. FGFR4 overexpression induced higher AZD4547 sensitivity in both models, as observed *in vitro*. The combination of both drugs showed high efficacy in all conditions, but the effects were more pronounced in both FGFR4-overexpressing models compared to control tumors.

Regarding downstream signaling, increased AKT, p42/p44 and STAT3 signaling was observed in the tumors with FGFR4 overexpression, in agreement with our earlier *in vitro* observations (Fig. 5**C**). In both FGFR4-overepressing H1975 and HCC827 models, FGFR inhibition by AZD4547 reduced the activation of the signaling pathways under examination. However, no such effects were observed in their control counterparts, suggesting that the effects of this inhibitor were specific for FGFR4 inhibition. In the tumors generated by H1975 xenografts, erlotinib alone caused only a modest inhibition of AKT and p42/p44 activation. However, its combination with AZD4547 potentiated these effects in the FGFR4-overexpressing tumors, resulting in a higher abrogation of oncogenic signaling. In the erlotinib-sensitive HCC827 cell lines, erlotinib monotherapy decreased activation of the AKT and p42/p44 pathways, with the combined therapy found to be even more effective at this, especially in the FGFR4-overexpressing condition. As observed *in vitro*, while erlotinib treatment boosted STAT3 activation in the HCC827 xenograft model, its combination with AZD4547 reversed this effect. These results suggest that combined

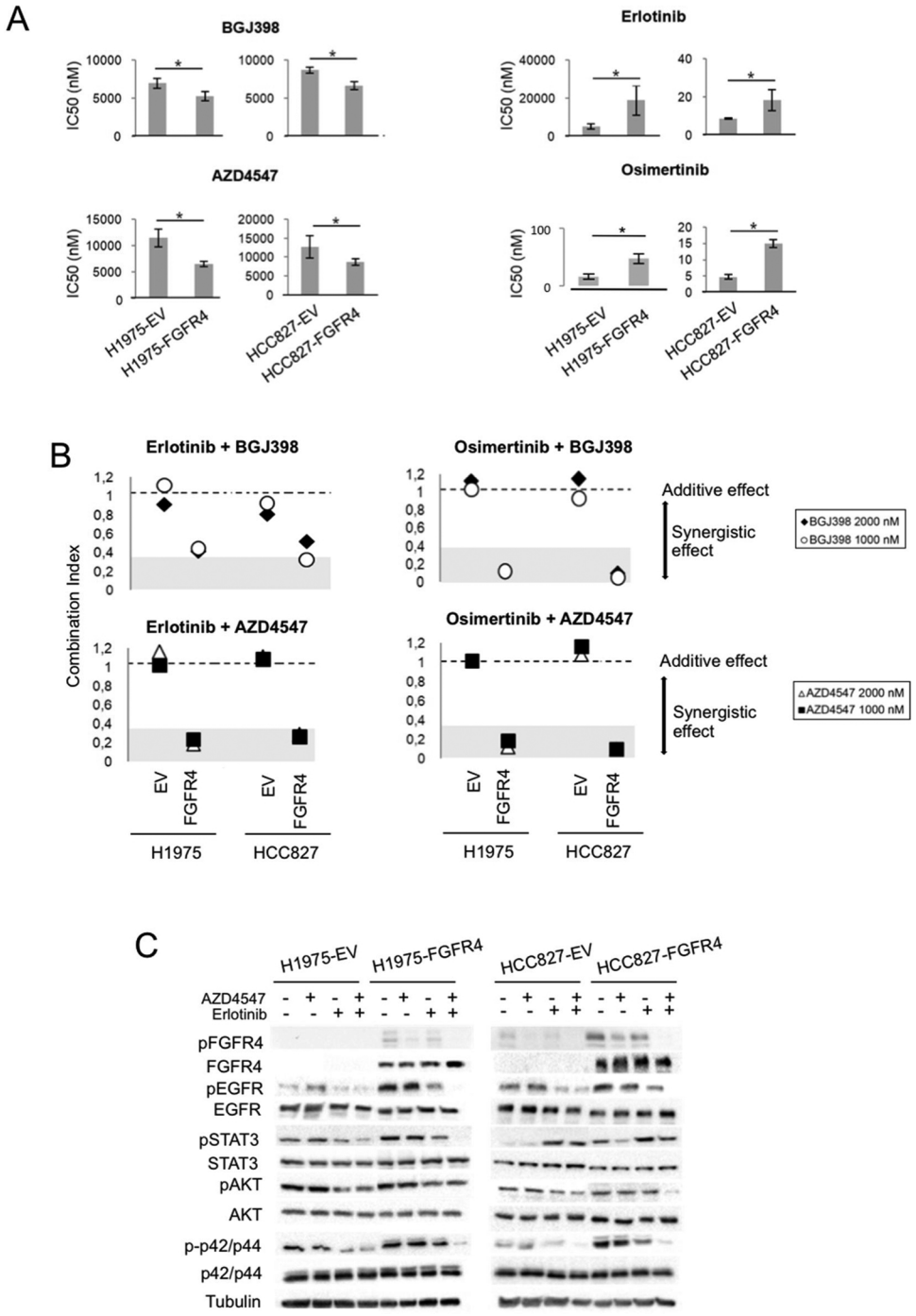

Fig. 4. *In vitro* effects of FGFR4 overexpression on EGFR and FGFR inhibitor sensitivity. (A) IC50 assays of the FGFR inhibitors BGJ398 and AZD4547 and EGFR inhibitors erlotinib and osimertinib in the H1975 and HCC827 cell lines, with or without overexpression of FGFR4. (B) Effects of the combination of EGFR- and FGFR-targeted therapies in these cell lines, assessed by the Combinatory Index (CI). The dashed line indicates the values (around CI = 1) where combination therapy has an additive effect. Values under this line (CI < 1) reflect synergism. The grey area limits the values showing strong synergism. (C) Effects of the combination of erlotinib and AZD4547 on pro-tumorigenic signaling in these cell lines. All experiments were reproduced a minimum of 3 times in the laboratory. In the IC50 assay results, the mean and standard deviation for the technical replicates are shown. Protein extraction was performed after a 24-hour treatment with the IC50 of erlotinib and 2 u M of AZD4547. For western blots, a representative image is shown, which is product of cropping from a larger blot image. EV = Empty vector control, FGFR4 = FGFR4-overexpressing. p-values were obtained with the two-sided Mann-Whitney U test and are indicated by asterisks (* $p < 0.05$; ** $p < 0.01$; *** $p < 0.001$) (For interpretation of the references to colour in this figure legend, the reader is referred to the web version of this article).

EGFR/FGFR inhibition could be an efficacious therapeutic approach for FGFR4-expressing, EGFR-activated adenocarcinoma tumors.

3.6. FGFR4 expression as a potential biomarker for EGFR inhibition efficacy

FGFR4 expression was determined at the mRNA level in a group of formalin-fixed, paraffin-embedded (FPPE) samples from a cohort of adenocarcinoma patients treated with erlotinib or gefitinib (**Supplementary table S2**, Fig. 5**D** N = 47). As our earlier results suggested that the cooperation between FGFR4 and EGFR was independent of EGFR activating mutations, we included EGFR-mutated and wild type samples in our analysis. We observed that patients with high FGFR4 expression exhibited poorer response to EGFR inhibition (HR 4.81 [2.24–10.34], $p < 0.001$), with similar results obtained when EGFR-mutated and wild type patients were analyzed independently (**Supplementary Figures S3 A-B**) When these analyses were repeated in an extended cohort including squamous and other NSCLC histological subtypes (N = 87, **Supplementary table S2**), similar results were obtained (HR 3.65 ([2.18–6.11], $p < 0.001$, **Supplementary Figure S3C**), suggesting that our results may be extendable to other NSCLC histologies. To rule out the possibility that the observed effects could be due to a prognostic role for FGFR4 expression in this setting, we performed the same analyses on the TCGA lung cancer cohort (**Supplementary Figure S3D**), which revealed no prognostic role for FGFR4 mRNA expression in NSCLC.

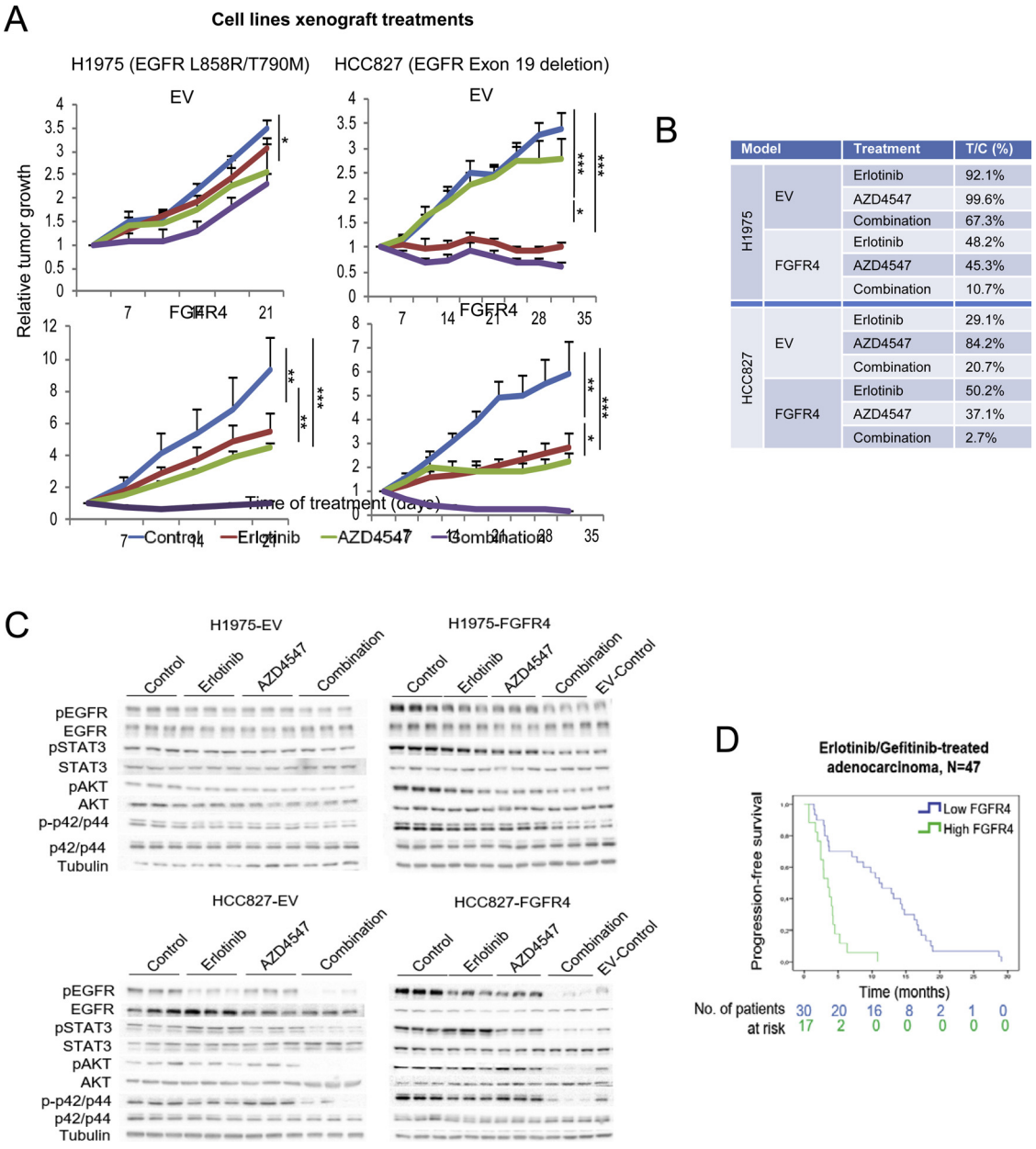

Model		Treatment	T/C (%)
H1975	EV	Erlotinib	92.1%
		AZD4547	99.6%
		Combination	67.3%
	FGFR4	Erlotinib	48.2%
		AZD4547	45.3%
		Combination	10.7%
HCC827	EV	Erlotinib	29.1%
		AZD4547	84.2%
		Combination	20.7%
	FGFR4	Erlotinib	50.2%
		AZD4547	37.1%
		Combination	2.7%

Fig. 5. Effect of dual EGFR and FGFR inhibition on cell line xenograft models. (A) Effect of erlotinib and AZD4547 on tumor growth in two EGFR-mutated adenocarcinoma cell line xenograft models, H1975 and HCC827, with or without FGFR4 overexpression. Relative tumor growth is shown, which was calculated as tumor volume increase from the beginning of the treatment. (B) Mean relative size of treated tumor groups compared to the untreated tumor control group (T/C), expressed as percentages. (C) Western blots showing the impact of treatment of H1975 and HCC827 xenograft models with or without FGFR4 overexpression, on the activation of pro-tumorigenic signaling. In the FGFR4-overexpressing xenograft western blots, one protein sample from the empty vector untreated control was added for comparison. (C) Effect of FGFR4 mRNA expression on progression-free survival of erlotinib- or gefitinib-treated lung adenocarcinoma patients (a description of the cohort is given in **Supplementary Table S2**). The cut-off value to define high or low expression was the median expression value for every gene. Two different erlotinib concentrations were used for these experiments: 50 mg/kg/day for the erlotinib-resistant models (H1975), and 20 mg/kg/day for the erlotinib-sensitive model (HCC827 xenograft). AZD4547 was administered at 5 mg/kg/day in every case. p-values were obtained with the two-sided Mann-Whitney U test and are indicated by asterisks (* $p < 0.05$; ** $p < 0.01$; *** $p < 0.001$). EV = Empty vector control, FGFR4 = FGFR4-overexpressing, T/C = Treated/control (For interpretation of the references to colour in this figure legend, the reader is referred to the web version of this article).

4. Discussion

We have provided evidence of a cooperative interaction between FGFR4 and EGFR in the context of EGFR-dependent lung adenocarcinoma, which is independent of EGFR activating mutations. This cooperation is likely to occur through a physical interaction between both receptors leading to their overactivation and to EGFR therapy resistance, as shown by our *in vitro*, *in vivo* and clinical evidence. In addition, we have shown that a combination of EGFR and FGFR inhibitors may offer an effective therapeutic approach for tumors with both high EGFR activation and FGFR4 expression.

Several examples in the literature describe cooperation between different RTKs in a variety of tumoral contexts, leading to therapy resistance similar to that described here. The IGF1R receptor, for instance, interacts with the insulin receptor in cell lines derived from gastric and liver tumors, correlating with higher AKT and STAT3 activation [28]. EGFR itself has been shown to physically interact with PDGFRβ in bladder cancer, and with IGFR1 in lung cancer, leading to

increased EGFR inhibitor resistance [29,30]. In fact, a potential relationship between EGFR and another member of the FGFR family, FGFR1, has been proposed in the head and neck carcinoma setting, which gives rise to FGFR inhibition resistance. In this work we have shown that FGFR4 interacts with EGFR and that when they are co-expressed, one is able to activate the other, leading to increased oncogenic signaling *in vitro* and *in vivo*. In line with our results, a previous report showed that FGFR4 expression is induced in MEFs transformed by EGFR overexpression, in contrast to MEFs transformed by other means [20]. FGFR4 overexpression in this context, as shown by our results, may further activate EGFR, which could confer a selective growth and tumorigenic advantage, thus providing an explanation for this observed phenotype. Furthermore, our results show that the EGFR-FGFR4 cooperation confers EGFR inhibition resistance *in vitro* and *in vivo*. Consistent with this, we have shown that FGFR4 expression is predictive of EGFR inhibition efficacy in NSCLC patients.

The role of other FGFR family members in EGFR inhibition resistance has been described in several published works, with FGFR1/FGFR2 upregulation as well as FGFR3 mutations known to be resistance mechanisms to anti-EGFR therapy [31–35], for which the combined use of EGFR and FGFR inhibitors has been proposed. Indeed, the inhibition of FGFR2 causes increased sensitivity to erlotinib *in vitro* in some lung cancer models [36]. However, we are the first to describe such a role for FGFR4. In addition, the previous studies were focused mainly on the role of these FGFRs in acquired resistance after EGFR inhibitor treatment. Nonetheless, we show that FGFR4 overexpression can occur in tumors before their exposure to EGFR inhibitors, leading to intrinsic anti-EGFR therapy resistance, as our patient cohort had not received previous EGFR inhibition therapy. Taken together, these findings suggest a potential close interaction between EGFR and FGFRs, which may be interesting to explore in order to identify other FGFRs in different tumoral settings.

At the therapeutic level, the logical approach to address the cooperation between FGFR4 and EGFR was the combined inhibition of both receptors. To explore the potential efficacy and specificity of this approach, we tested the effect of FGFR and EGFR inhibitors in monotherapy or in combination in syngeneic models with FGFR4 overexpression *in vitro* and *in vivo*. We found that the combined inhibition showed superior and dramatic effects in terms of proliferation or tumor growth than when either inhibitor was used alone, especially in models with induced FGFR4 expression, thereby demonstrating the potential efficacy of this combined treatment in EGFR-activated, FGFR4-expressing tumors. These results suggest that dual EGFR/FGFR inhibition may serve as a potentially effective therapy for patients with high EGFR activation and FGFR4 expression.

To the present time, the use of EGFR inhibitors has been limited to adenocarcinoma tumors with known EGFR activating mutations. In this work, we provide evidence that the EGFR-FGFR4 cooperativity described here is independent of EGFR-activating mutations. Correlating with this observation, when we independently analyzed the response of tumors to EGFR inhibition in our cohort of erlotinib/gefitinib-treated adenocarcinoma patients (EGFR wild type and mutated), we found that FGFR4 expression was equally predictive of response in these subsets of patients. Furthermore, when these analyses were performed in an extended cohort including patients from all NSCLC histologies, similar results were obtained. Taken together, these findings suggest that the efficacy of the combination EGFR/FGFR inhibition therapy may be extended to EGFR-wild type tumors from any NSCLC histological subtype, as long as they exhibit high EGFR activation and FGFR4 expression. However, more experiments are required to confirm this possibility.

5. Conclusions

The assessment of FGFR4 expression may be predictive for EGFR inhibition efficacy in EGFR-mutated and wild type NSCLC tumors. Furthermore, the determination of both FGFR4 expression and EGFR activation may be selective for patients who will benefit from combined EGFR/FGFR inhibition therapy. Thus, we propose a novel predictive biomarker for EGFR therapy, and an effective therapeutic approach for a subset of tumors with EGFR dependence, exhibiting high FGFR4 expression. In addition, we present the molecular criteria needed to select patients who will likely respond to this combined therapy.

DECLARATIONS

Ethics approval and consent to participate

Written informed consent was provided by all patients. The project was approved by the Research Ethics Committee of the Hospital Universitario 12 de Octubre (Madrid, Spain) (CEI 16/297).

The procedures involving animals were approved by the Animal Protection Committee of the Comunidad Autónoma de Madrid (Approval ID: PROEX134/16).

Authors' contributions

Conceptualization, A.Q., I.F., S.M.P., A.C., and L.P.A.; Methodology, A.Q., A.C., I.F., A.B.E and S.M.P.; Investigation, A.Q., A.C., I.F., L.P.A. and S.M.P.; Validation, A.Q., A.M, P.Y., L.O., R.S., A.M., and L.O.; Formal Analysis, A.Q., I.F., S.P., L.M., and E.C., Writing – Original Draft, A.Q., I.F., A.C., S.M.P. and L.P.A., Writing – Review & Editing, A.Q., I.F., A.C., S.M.P. and L.P.A., Supervision, A.C., I.F., S.M.P., and L.P.A.; Funding Acquisition, S.M.P., I.F. and L.P.A.

Funding

L.P.A. was funded by the Comunidad de Madrid, CAM, (B2017/BMD3884), ISCIII (PI14/01964, PIE15/00076, PI17/00778 and DTS17/00089) and CIBERONC (CD16/12/00442), and co-funded by FEDER from Regional Development European Funds (European Union). I.F. is funded by the AECC (AIO2015) and Consejería de Igualdad, Salud y Políticas Sociales de la Junta de Andalucía (PI-0029-2013) and ISCIII (PI16/01311), and co-funded by FEDER from Regional Development European Funds (European Union). AC was supported by grants from the Spanish Ministry of Economy and Competitiveness Plan Estatal de I + D + I 2013–2016, ISCIII (PI15/00045) and CIBERONC (CD16/12/00275), and co-funded by FEDER from Regional Development European Funds (European Union). S.M.P. is funded by the Consejería de Salud y Bienestar Social (PI-0046-2012), the Fundación Mutua Madrileña (2014) and ISCIII (PI17/00033). A.Q is funded by the ISCIII (FI12/00429). L.O. is funded by the Ministerio de Educación, Cultura y Deporte (FPU13/02595).

Acknowledgements

The authors thank the CNIO Confocal Microscopy Unit for their specialist assistance and support. The authors also thank the donors and the Hospital 12 de Octubre Biobank for the human specimens used in this study.

Appendix A. Supplementary data

Supplementary material related to this article can be found, in the online version, at doi:https://doi.org/10.1016/j.lungcan.2019.02.007.

References

[1] R.L. Siegel, K.D. Miller, A. Jemal, Cancer Statistics, CA Cancer J. Clin. 67 (1) (2017) 7–30 2017.

[2] M. Cabanero, R. Sangha, B.S. Sheffield, M. Sukhai, M. Pakkal, S. Kamel-Reid, A. Karsan, D. Ionescu, R.A. Juergens, C. Butts, M.S. Tsao, Management of EGFR-mutated non-small-cell lung cancer: practical implications from a clinical and pathology perspective, Curr. Oncol. 24 (2) (2017) 111–119.

[3] D. Morgensztern, K. Politi, R.S. Herbst, EGFR mutations in non-small-Cell lung Cancer: find, divide, and conquer, JAMA Oncol. 1 (2) (2015) 146–148.
[4] F. Passiglia, A. Listi, M. Castiglia, A. Perez, S. Rizzo, V. Bazan, A. Russo, EGFR inhibition in NSCLC: New findings…. and opened questions? Crit. Rev. Oncol. Hematol. 112 (2017) 126–135.
[5] A.L. Moreira, J. Eng, Personalized therapy for lung cancer, Chest 146 (6) (2014) 1649–1657.
[6] S. Li, Y.L. Choi, Z. Gong, X. Liu, M. Lira, Z. Kan, E. Oh, J. Wang, J.C. Ting, X. Ye, C. Reinhart, X. Liu, Y. Pei, W. Zhou, R. Chen, S. Fu, G. Jin, A. Jiang, J. Fernandez, J. Hardwick, M.W. Kang, H. I, H. Zheng, J. Kim, M. Mao, Comprehensive characterization of oncogenic drivers in asian lung adenocarcinoma, J. Thorac. Oncol. 11 (12) (2016) 2129–2140.
[7] T.M. Brand, M. Iida, C. Li, D.L. Wheeler, The nuclear epidermal growth factor receptor signaling network and its role in cancer, Discov. Med. 12 (66) (2011) 419–432.
[8] R. Gupta, A.M. Dastane, R. McKenna Jr., A.M. Marchevsky, The predictive value of epidermal growth factor receptor tests in patients with pulmonary adenocarcinoma: review of current "best evidence" with meta-analysis, Hum. Pathol. 40 (3) (2009) 356–365.
[9] S. Kobayashi, T.J. Boggon, T. Dayaram, P.A. Janne, O. Kocher, M. Meyerson, B.E. Johnson, M.J. Eck, D.G. Tenen, B. Halmos, EGFR mutation and resistance of non-small-cell lung cancer to gefitinib, N. Engl. J. Med. 352 (8) (2005) 786–792.
[10] A. Quintanal-Villalonga, L. Paz-Ares, I. Ferrer, S. Molina-Pinelo, Tyrosine Kinase Receptor Landscape in Lung Cancer: Therapeutical Implications, Dis. Markers 2016 (2016) 9214056.
[11] A. Inoue, K. Yoshida, S. Morita, F. Imamura, T. Seto, I. Okamoto, K. Nakagawa, N. Yamamoto, S. Muto, M. Fukuoka, Characteristics and overall survival of EGFR mutation-positive non-small cell lung cancer treated with EGFR tyrosine kinase inhibitors: a retrospective analysis for 1660 Japanese patients, Jpn. J. Clin. Oncol. 46 (5) (2016) 462–467.
[12] J.Y. Yu, S.F. Yu, S.H. Wang, H. Bai, J. Zhao, T.T. An, J.C. Duan, J. Wang, Clinical outcomes of EGFR-TKI treatment and genetic heterogeneity in lung adenocarcinoma patients with EGFR mutations on exons 19 and 21, Chin. J. Cancer 35 (2016) 30.
[13] I. Ferrer, A. Quintanal-Villalonga, S. Molina-Pinelo, J.M. Garcia-Heredia, M. Perez, R. Suarez, S. Ponce-Aix, L. Paz-Ares, A. Carnero, MAP17 predicts sensitivity to platinum-based therapy, EGFR inhibitors and the proteasome inhibitor bortezomib in lung adenocarcinoma, J. Exp. Clin. Cancer Res. 37 (1) (2018) 195.
[14] H.P. Huang, H. Feng, H.B. Qiao, Z.X. Ren, G.D. Zhu, The prognostic significance of fibroblast growth factor receptor 4 in non-small-cell lung cancer, Onco. Ther. 8 (2015) 1157–1164.
[15] L. Ding, G. Getz, D.A. Wheeler, E.R. Mardis, M.D. McLellan, K. Cibulskis, C. Sougnez, H. Greulich, D.M. Muzny, M.B. Morgan, L. Fulton, R.S. Fulton, Q. Zhang, M.C. Wendl, M.S. Lawrence, D.E. Larson, K. Chen, D.J. Dooling, A. Sabo, A.C. Hawes, H. Shen, S.N. Jhangiani, L.R. Lewis, O. Hall, Y. Zhu, T. Mathew, Y. Ren, J. Yao, S.E. Scherer, K. Clerc, G.A. Metcalf, B. Ng, A. Milosavljevic, M.L. Gonzalez-Garay, J.R. Osborne, R. Meyer, X. Shi, Y. Tang, D.C. Koboldt, L. Lin, R. Abbott, T.L. Miner, C. Pohl, G. Fewell, C. Haipek, H. Schmidt, B.H. Dunford-Shore, A. Kraja, S.D. Crosby, C.S. Sawyer, T. Vickery, S. Sander, J. Robinson, W. Winckler, J. Baldwin, L.R. Chirieac, A. Dutt, T. Fennell, M. Hanna, B.E. Johnson, R.C. Onofrio, R.K. Thomas, G. Tonon, B.A. Weir, X. Zhao, L. Ziaugra, M.C. Zody, T. Giordano, M.B. Orringer, J.A. Roth, M.R. Spitz, I.I. Wistuba, B. Ozenberger, P.J. Good, A.C. Chang, D.G. Beer, M.A. Watson, M. Ladanyi, S. Broderick, A. Yoshizawa, W.D. Travis, W. Pao, M.A. Province, G.M. Weinstock, H.E. Varmus, S.B. Gabriel, E.S. Lander, R.A. Gibbs, M. Meyerson, R.K. Wilson, Somatic mutations affect key pathways in lung adenocarcinoma, Nature 455 (7216) (2008) 1069–1075.
[16] A. Quintanal-Villalonga, A. Carranza-Carranza, R. Melendez, I. Ferrer, S. Molina-Pinelo, L. Paz-Ares, Prognostic role of the FGFR4-388Arg variant in lung squamous-cell carcinoma patients with lymph node involvement, Clin. Lung Cancer 18 (6) (2017) 667–674 e1.
[17] A. Quintanal-Villalonga, L. Ojeda-Marquez, A. Marrugal, P. Yague, S. Ponce-Aix, A. Salinas, A. Carnero, I. Ferrer, S. Molina-Pinelo, L. Paz-Ares, The FGFR4-388arg variant promotes lung Cancer progression by N-Cadherin induction, Sci. Rep. 8 (1) (2018) 2394.
[18] A. Quintanal-Villalonga, M. Mediano, I. Ferrer, R. Melendez, A. Carranza-Carranza, R. Suarez, A. Carnero, S. Molina-Pinelo, L. Paz-Ares, Histology-dependent prognostic role of pERK and p53 protein levels in early-stage non-small cell lung cancer, Oncotarget 9 (28) (2018) 19945–19960.
[19] Z.Y. Yang, M.Y. Di, J.Q. Yuan, W.X. Shen, D.Y. Zheng, J.Z. Chen, C. Mao, J.L. Tang, The prognostic value of phosphorylated Akt in breast cancer: a systematic review, Sci. Rep. 5 (2015) 7758.
[20] N. Seitzer, T. Mayr, S. Streit, A. Ullrich, A single nucleotide change in the mouse genome accelerates breast cancer progression, Cancer Res. 70 (2) (2010) 802–812.
[21] M.V. Guijarro, J.F. Leal, C. Blanco-Aparicio, S. Alonso, J. Fominaya, M. Lleonart, J. Castellvi, S. Ramon y Cajal, A. Carnero, MAP17 enhances the malignant behavior of tumor cells through ROS increase, Carcinogenesis 28 (10) (2007) 2096–2104.
[22] V. Moneo, B.G. Serelde, C. Blanco-Aparicio, R. Diaz-Uriarte, P. Aviles, G. Santamaria, J.C. Tercero, C. Cuevas, A. Carnero, Levels of active tyrosine kinase receptor determine the tumor response to Zalypsis, BMC Cancer 14 (2014) 281.
[23] T.C. Chou, Drug combination studies and their synergy quantification using the Chou-Talalay method, Cancer Res. 70 (2) (2010) 440–446.
[24] I. Ferrer, C. Blanco-Aparicio, S. Peregrina, M. Canamero, J. Fominaya, Y. Cecilia, M. Lleonart, J. Hernandez-Losa, S. Ramon y Cajal, A. Carnero, Spinophilin acts as a tumor suppressor by regulating Rb phosphorylation, Cell Cycle 10 (16) (2011) 2751–2762.
[25] L.M. McShane, D.G. Altman, W. Sauerbrei, S.E. Taube, M. Gion, G.M. Clark, REporting recommendations for tumor MARKer prognostic studies (REMARK), Nat. Clin. Pract. Urol. 2 (8) (2005) 416–422.
[26] E. Manchado, S. Weissmueller, J.Pt. Morris, C.C. Chen, R. Wullenkord, A. Lujambio, E. de Stanchina, J.T. Poirier, J.F. Gainor, R.B. Corcoran, J.A. Engelman, C.M. Rudin, N. Rosen, S.W. Lowe, A combinatorial strategy for treating KRAS-mutant lung cancer, Nature 534 (7609) (2016) 647–651.
[27] H.J. Lee, G. Zhuang, Y. Cao, P. Du, H.J. Kim, J. Settleman, Drug resistance via feedback activation of Stat3 in oncogene-addicted cancer cells, Cancer Cell 26 (2) (2014) 207–221.
[28] J.G. Kim, M.J. Kang, Y.K. Yoon, H.P. Kim, J. Park, S.H. Song, S.W. Han, J.W. Park, G.H. Kang, K.W. Kang, D.Y. Oh, S.A. Im, Y.J. Bang, E.C. Yi, T.Y. Kim, Heterodimerization of glycosylated insulin-like growth factor-1 receptors and insulin receptors in cancer cells sensitive to anti-IGF1R antibody, PLoS One 7 (3) (2012) e33322.
[29] P.C. Black, G.A. Brown, C.P. Dinney, W. Kassouf, T. Inamoto, A. Arora, D. Gallagher, M.F. Munsell, M. Bar-Eli, D.J. McConkey, L. Adam, Receptor heterodimerization: a new mechanism for platelet-derived growth factor induced resistance to anti-epidermal growth factor receptor therapy for bladder cancer, J. Urol. 185 (2) (2011) 693–700.
[30] F. Morgillo, J.K. Woo, E.S. Kim, W.K. Hong, H.Y. Lee, Heterodimerization of insulin-like growth factor receptor/epidermal growth factor receptor and induction of survivin expression counteract the antitumor action of erlotinib, Cancer Res. 66 (20) (2006) 10100–10111.
[31] K. Azuma, A. Kawahara, K. Sonoda, K. Nakashima, K. Tashiro, K. Watari, H. Izumi, M. Kage, M. Kuwano, M. Ono, T. Hoshino, FGFR1 activation is an escape mechanism in human lung cancer cells resistant to afatinib, a pan-EGFR family kinase inhibitor, Oncotarget 5 (15) (2014) 5908–5919.
[32] H. Terai, K. Soejima, H. Yasuda, S. Nakayama, J. Hamamoto, D. Arai, K. Ishioka, K. Ohgino, S. Ikemura, T. Sato, S. Yoda, R. Satomi, K. Naoki, T. Betsuyaku, Activation of the FGF2-FGFR1 autocrine pathway: a novel mechanism of acquired resistance to gefitinib in NSCLC, Mol. Cancer Res. 11 (7) (2013) 759–767.
[33] K.E. Ware, T.K. Hinz, E. Kleczko, K.R. Singleton, L.A. Marek, B.A. Helfrich, C.T. Cummings, D.K. Graham, D. Astling, A.C. Tan, L.E. Heasley, A mechanism of resistance to gefitinib mediated by cellular reprogramming and the acquisition of an FGF2-FGFR1 autocrine growth loop, Oncogenesis 2 (2013) e39.
[34] A.S. Crystal, A.T. Shaw, L.V. Sequist, L. Friboulet, M.J. Niederst, E.L. Lockerman, R.L. Frias, J.F. Gainor, A. Amzallag, P. Greninger, D. Lee, A. Kalsy, M. Gomez-Caraballo, L. Elamine, E. Howe, W. Hur, E. Lifshits, H.E. Robinson, R. Katayama, A.C. Faber, M.M. Awad, S. Ramaswamy, M. Mino-Kenudson, A.J. Iafrate, C.H. Benes, J.A. Engelman, Patient-derived models of acquired resistance can identify effective drug combinations for cancer, Science 346 (6216) (2014) 1480–1486.
[35] K.E. Ware, M.E. Marshall, L.R. Heasley, L. Marek, T.K. Hinz, P. Hercule, B.A. Helfrich, R.C. Doebele, L.E. Heasley, Rapidly acquired resistance to EGFR tyrosine kinase inhibitors in NSCLC cell lines through de-repression of FGFR2 and FGFR3 expression, PLoS One 5 (11) (2010) e14117.
[36] B. Dai, S. Yan, H. Lara-Guerra, H. Kawashima, R. Sakai, G. Jayachandran, M. Majidi, R. Mehran, J. Wang, B.N. Bekele, V. Baladandayuthapani, S.Y. Yoo, Y. Wang, J. Ying, F. Meng, L. Ji, J.A. Roth, Exogenous Restoration of TUSC2 Expression Induces Responsiveness to Erlotinib in Wildtype Epidermal Growth Factor Receptor (EGFR) Lung Cancer Cells through Context Specific Pathways Resulting in Enhanced Therapeutic Efficacy, PLoS One 10 (6) (2015) e0123967.